The Impact of the Eccentricity of the Tension Pulley on the Dynamic Response of the Stacker Superstructure

Marko Urošević
Research Assistant
University of Belgrade
Faculty of Mechanical Engineering

Nenad Zrnić
Professor
University of Belgrade
Faculty of Mechanical Engineering

Stackers are one of the vital parts of the system that work on the exploitation of coal in open-pit mines. During their exploitation life, they are exposed to hard working conditions in which dynamic and stochastic loads act on them. Therefore, the analysis of their dynamic behavior is necessary in order to prevent failures and ensure a longer working life. Given that the structure of the stackers is a dominantly spatial truss structure, the paper presents the procedure of forming a spatial reduced dynamic model of the stacker superstructure and analysis of the influence of the eccentricity of the discharge boom tension pulley created during the production process. The results are given through the displacements and accelerations of the referent points of the structure. The quantification of the eccentricity influence from the aspect of the dynamic behaviour of the machine is presented and discussed.

Keywords: *Stacker, reduced dynamic model, tension pulley eccentricity, dynamic response*

1. INTRODUCTION

The problem of mechanical resonance was observed three hundred years ago [1], but it got its true importance and application in the field of machines for continuous and cycling material handling only in the 20th century. [2-10] Due to their impact on the GDP, the economic stability of the country, as well as the still high dependence of the energy sector of many countries on coal, mega machines that work on open-pit mines, stand out. Serbia is included in these countries, whose electricity production is still dominantly dependent on thermal power plants and where around 70% of electricity production comes from lignite. [11, 12] According to the projected energy consumption in Serbia, its lignite reserves are sufficient to provide it until the end of the 21st century. [13]

The backbone of lignite production is open-pit mines where it is exploited, transported, processed, and shipped to thermal power plants. Their core presents machines for continuous excavation, transport, and handling of materials. In order to use the capacity of these machines, they are subjected to work in extremely difficult conditions 24/7, during which forces of a dynamic and stochastic character act on them. [14] However, frequent stoppages and failures [15, 16] of certain subsystems of these machines prevent a high percentage of their time utilization. [17]. On the other hand, bearing in mind that these machines work in a serially coupled systems, this results in high economic losses, because the stoppage of one machine inevitably means the stoppage of the entire system. [15]

Correspondence to: Marko Urošević, Research Assistant
Faculty of Mechanical Engineering,
Kraljice Marije 16, 11120 Belgrade 35, Serbia
E-mail: murosevic@mas.bg.ac.rs

One of the machines of this type is stackers, whose role is the continuous transfer of materials to coal and overburden landfills. During their exploitation life, stackers are exposed to dynamic loads due to uneven flow of material, impacts of material at transshipment points, and imbalance of end pulleys and conveyor rollers. [18]. Understanding the impact of these loads on the dynamic behavior of the stackers would ensure both an extension of their working life and a higher percentage of their time utilization. Due to the geometric complexity and stochastic nature of the loading of this type of machine, in order to determine the dynamic characteristics, researchers generally resort to experimental measurements [19, 20]. The lack of experimental measurements is reflected in their economic impact because they often require stopping the production process, the impossibility of being performed, and they can only be performed on machines that are already in the period of exploitation. On the other hand, the development of a reduced dynamic model overcomes these shortcomings, and one of its main advantages is that it can be applied already at the design stage, however, due to its complex mathematical formulation, it is often omitted from the analysis, as shown by the fact that even the relevant technical regulation from this field dynamic influences considered as static loads multiplied by a certain factor. [21-23]

The tension pulley of the discharge boom conveyor is located at its top, therefore, when there is an eccentricity of its axis of rotation, additional periodic inertial forces appear which can lead to an oscillation of the structure. In the case of resonance, these oscillations can cause significant dynamic loads. In [24], the activation of the belt conveyor drive was used as the only excitation to determine the natural frequencies of the stacker "DQLZ 1200".

Below is presented the procedure of mathematical formulation of the spatial reduced dynamic model of the stacker superstructure and the analysis of the response of the system to the excitation load caused by the imbalance

of the tension pulley of the discharge boom conveyor, as well as the quantification of the impact caused by this load.

2. SPATIAL REDUCED DYNAMIC MODEL

The spatial reduced dynamic model [25] is a mathematical model that takes into account the deformability of the system, the arrangement of continuously distributed and concentrated masses, and the excitation loads of the system, in relation to the selected generalized coordinates. As such, it provides an insight into the dynamic behavior, that is, the response of the system to a defined excitation load, while providing the possibility of varying the structural parameters of the observed system. Considering the complexity of the stacker superstructure system, the differential equations of motion of the reduced dynamic model were formed according to the Lagrangian equations of the second order

$$\frac{d}{dt}\left(\frac{\partial T}{\partial \dot{q}_j}\right)+\frac{\partial \Pi}{\partial q_j}=Q_{\Omega j}(t),(j=1,2,\ldots,s), \qquad (1)$$

that is, in matrix form

$$\mathbf{A}\ddot{\mathbf{q}}+\mathbf{C}\mathbf{q}=\mathbf{Q}_{\Omega}(t), \qquad (2)$$

where: $\mathbf{A}$ is the matrix of inertia of the system, $\ddot{\mathbf{q}}$ is the vector of generalized accelerations of the system, $\mathbf{C}$ is the stiffness matrix of the system, $\mathbf{q}$ is the vector of generalized displacements of the system, $\mathbf{Q}_{\Omega}(t)$ is the vector of external non-potential forces.

The dimensions of the above-mentioned matrices are defined by the number of generalized coordinates, in the specific case, the reduced dynamic model consists of 42 generalized coordinates, distributed in 14 referent points (RPs) of the system, Figure 1. Adequate choice of generalized coordinates depends on the expected results that the model should provide. [26, 27] In the presented case, the model should enable adequate connection of the substructures of the stacker, adequate entry of external periodic loads, provide insight into the modal characteristics, and response of the system to the defined excitation load.

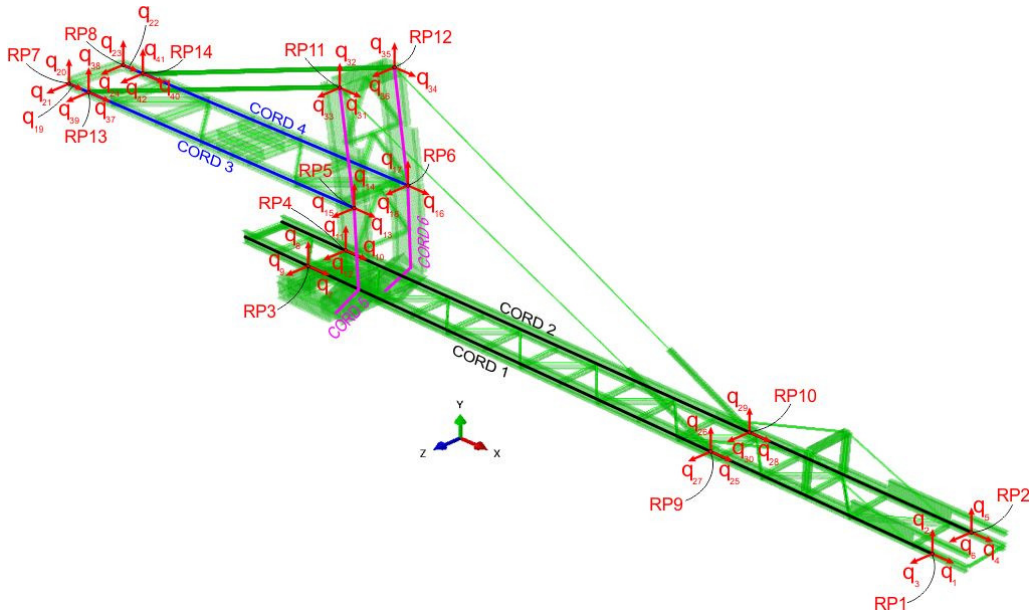

Figure 1. The spatial reduced dynamic model of the stacker superstructure

In order to determine the stiffness matrix of the system, a finite element (FE) model of the stacker superstructure was formed, Figure 2. The stiffness matrix is determined according to Clapeyron's theorem and represents the response of the FE model to unit loads acting in RPs in the directions of generalized coordinates.

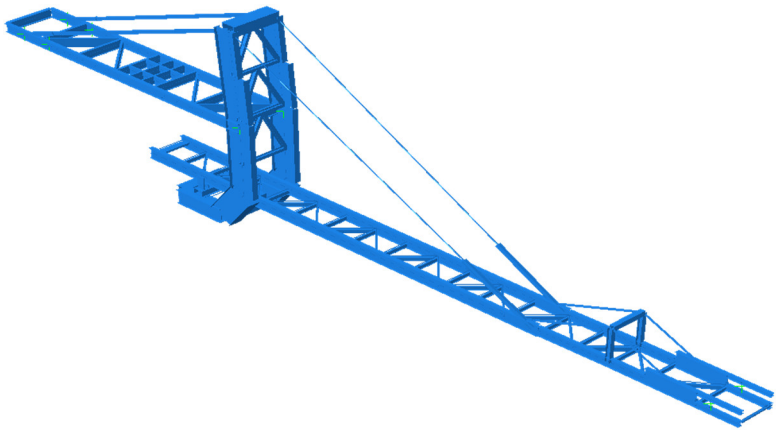

Figure 2. FE model of the stacker superstructure

As the potential energy of the observed system has the form

$$\Pi_{\text{stacker}} = \frac{1}{2}\mathbf{q}^{\mathrm{T}}\boldsymbol{\alpha}_{\text{stacker}}^{-1}\mathbf{q} = \frac{1}{2}\mathbf{q}^{\mathrm{T}}\mathbf{C}_{\text{stacker}}\mathbf{q}, \quad (3)$$

follows

$$\boldsymbol{\alpha}_{\text{stacker}}^{-1} = \mathbf{C}_{\text{stacker}}, \quad (4)$$

where $\boldsymbol{\alpha}_{\text{stacker}}$ is the flexibility matrix and $\mathbf{C}_{\text{stacker}}$ is the stiffness matrix of the system.

The matrix of inertia is determined through the kinetic energy of the system. The detailed procedure used to create an observed reduced model of the stacker superstructure is shown in [27].

The response of the system was analyzed for the excitation load that occurs due to the eccentricity of the tension pulley of the discharge boom conveyor. The eccentricity of the pulley can occur for several reasons, due to mistakes made during the production process itself, mistakes during assembly, uneven sticking of materials, and uneven wear of the pulley during exploitation. [18] In this case, the impact on the dynamic behavior of the structure due to the eccentricity created during the pulley production process and which is located in the plane of symmetry of the discharge boom was considered.

[28] divides pulleys into two types, general-purpose pulleys and machined pulleys intended for belts with a high modulus of elasticity. Permissible deviations of the axis of rotation depending on their diameter are defined for both types of pulleys and are shown in Table 1 and Table 2, respectively.

Table 1. Permissible Runout Tolerances for Common Applications [28]

Diameter, inch (mm)	Maximum Total Indicator Reading, inch (mm)
8-24 (≈ 200 - ≈ 610)	0.125 (3.175)
30-48 (≈ 760 - ≈ 1220)	0.188 (4.775)
54-60 (≈ 1370 - ≈ 1520)	0.250 (6.350)

Table 2. Permissible Runout Tolerances for High Modulus Belts [28]

Type	Maximum Total Indicator Reading, inch (mm)
Unlagged Pulley	0.030 (0.762)
Lagged pulley (under lagging)	0.030 (0.762)
Lagged pulley (over lagging)	0.030 (0.762)

As the angular frequency of the pulleys is

$$\Omega_{\text{pulley}} = \frac{\mathrm{V}_{\text{belt}}}{\mathrm{r}_{\text{pulley}}} = 12\ \frac{\text{rad}}{s}, \quad (5)$$

where $\mathrm{V}_{\text{belt}} = 6\frac{\text{m}}{\text{s}}$ is the speed of the belt of the discharge boom conveyor and $\mathrm{r}_{\text{pulley}} = 0.5$ m is the radius of the tension pulley, the frequency of excitation can be calculated as

$$\mathrm{f}_{\text{exc}} = \frac{\Omega_{\text{pulley}}}{2 \cdot \pi} = 1.91 \text{ Hz}. \quad (6)$$

As a consequence of the eccentricity of the pulley, an additional inertial load occurs in the form of centrifugal force $F_{\text{CF,exc}}$, Figure 3.

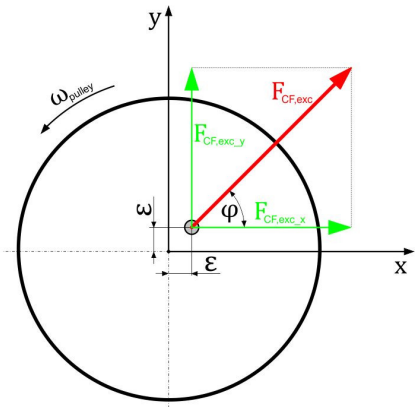

Figure 3. Loading scheme due to eccentricity of the pulley

The amplitude of the inertial force is equal

$$\mathrm{F}_{\text{CF,exc}} = \Omega_{\text{pulley}}^2 \mathrm{m}_{\text{pulley}} \varepsilon, \quad (7)$$

where $\mathrm{m}_{\text{pulley}} = 1079$ kg is the mass of the pulley, ε is the eccentricity of the pulley.

Considering (7), the excitation load has the form [18]

$$F_{\text{CF,exc}}(t) = \mathrm{F}_{\text{CF,exc}} \sin\left(\Omega_{\text{pulley}} t\right). \quad (8)$$

The components of the excitation load in the x axis (longitudinal axis of the discharge boom) and y axis (transverse axis of the discharge boom), according to Figure 3, can be written as

$$F_{\text{CF,exc\_x}}(t) = \Omega_{\text{pulley}}^2 m_{\text{pulley}} \varepsilon \cos\left(\varphi(t)\right), \quad (9)$$

$$F_{\text{CF,exc\_y}}(t) = \Omega_{\text{pulley}}^2 m_{\text{pulley}} \varepsilon \sin\left(\varphi(t)\right), \quad (10)$$

where $\varphi(t) = \Omega_{\text{pulley}} t$ is the angle that the inertial force overlaps with the x axis.

Now, the vector of generalized non-potential forces has the form

$$\mathbf{Q}_{\Omega}(t) = \mathbf{F}_{\text{x}}(t) + \mathbf{F}_{\text{y}}(t), \quad (11)$$

where $\mathbf{F}_{\text{x}}(t)$ is the excitation load vector in the x axis direction, $\mathbf{F}_{\text{y}}(t)$ is the excitation load vector in the y axis direction.

Based on the previously presented and (2) it can be shown that the vector of generalized displacements and the vector of generalized accelerations have the following form, respectively

$$\mathbf{q}_{\text{stacker}}(t) = \left[\mathbf{C}_{\text{stacker}} - \Omega_{\text{pulley}}^2 \mathbf{M}_{\text{stacker}}\right]^{-1} \cdot \mathbf{Q}_{\Omega}(t), \quad (12)$$

$$\ddot{\mathbf{q}}_{\text{stacker}}(t) = -\Omega_{\text{pulley}}^2 \left[\mathbf{C}_{\text{stacker}} - \Omega_{\text{pulley}}^2 \mathbf{M}_{\text{stacker}}\right]^{-1} \cdot \mathbf{Q}_{\Omega}(t), \quad (13)$$

where $\mathbf{M}_{\text{stacker}}$ is matrix of inertia of the system.

In order to quantify the influence of the eccentricity of the tension pulley on the dynamic behavior of the structure, the results obtained for five different values of

eccentricity were analyzed, $\varepsilon_1 = \varepsilon_{min} = 0.955$ mm, $\varepsilon_2 = 1.910$ mm, $\varepsilon_3 = 2.865$ mm, $\varepsilon_4 = 3.820$ mm, $\varepsilon_5 = \varepsilon_{max} = 4.775$ mm.

Figure 4 shows the diagrams of changes in inertial force components ($F_{CF,exc\_x}(t)$ and $F_{CF,exc\_y}(t)$) in time, depending on the eccentricity value.

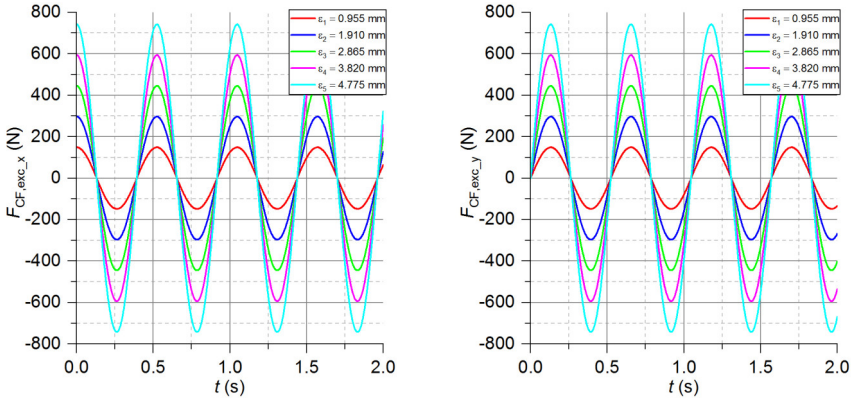

Figure 4. Diagrams of changes in inertial force components

3. RESULTS

Considering the lack of experimental results and the fact that the value frequency of excitation is closest to the value of the sixth natural frequency of the reduce dynamic (RD) model, the validation of the RD model was performed by comparing its first six natural frequencies (Table 3) and modal shapes with those obtained by the FE model (Figure 5). [27]

Table 3. Comparison of natural frequencies obtained by the FE and the reduced dynamic model

f_i	FE model - f_{FE} (Hz)	RD model - f_{RD} (Hz)	$(f_{RD} - f_{FE})/f_{RD} \cdot 100$ (%)
f_1	0.256	0.260	1.54
f_2	0.315	0.326	3.37
f_3	0.730	0.754	3.18
f_4	0.823	0.889	7.42
f_5	1.402	1.454	3.58
f_6	1.750	1.842	4.99

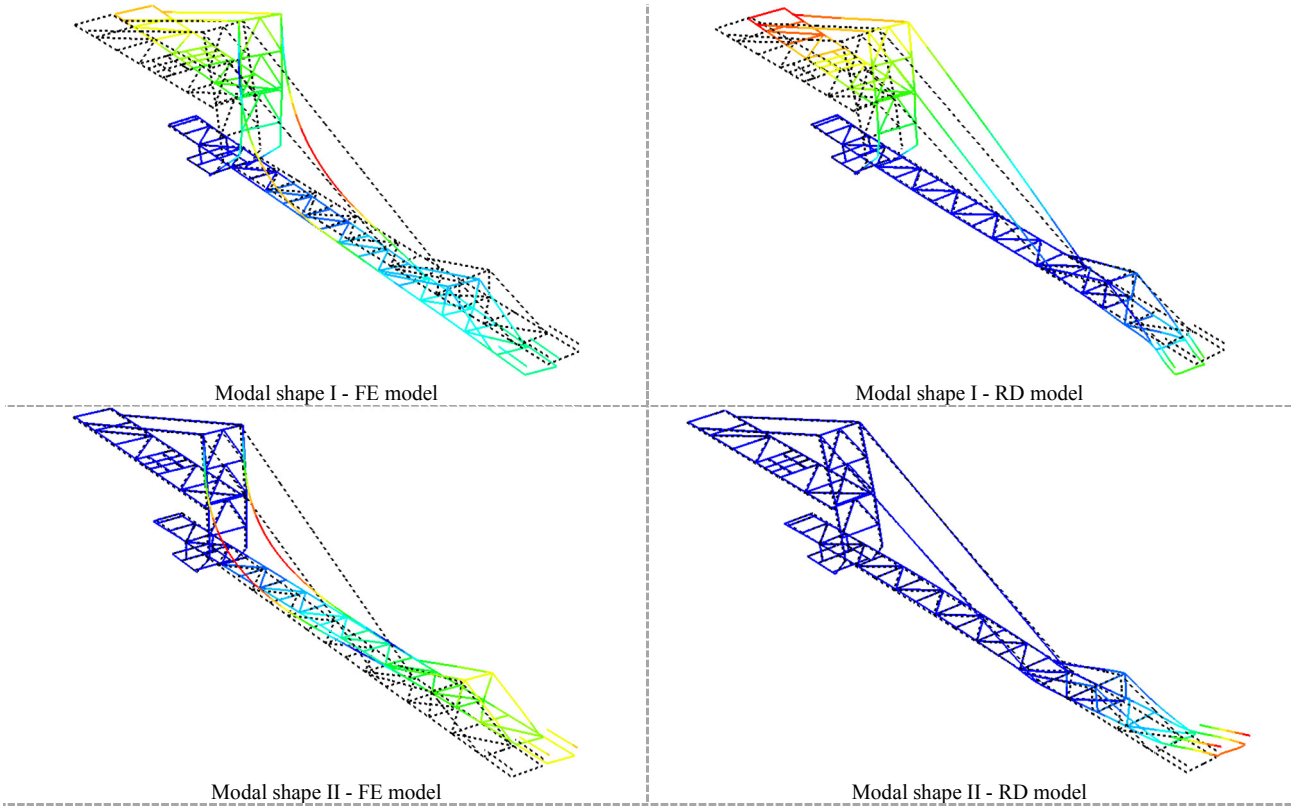

Figure 5. Comparison of FE and RD model modal shapes (part 1)

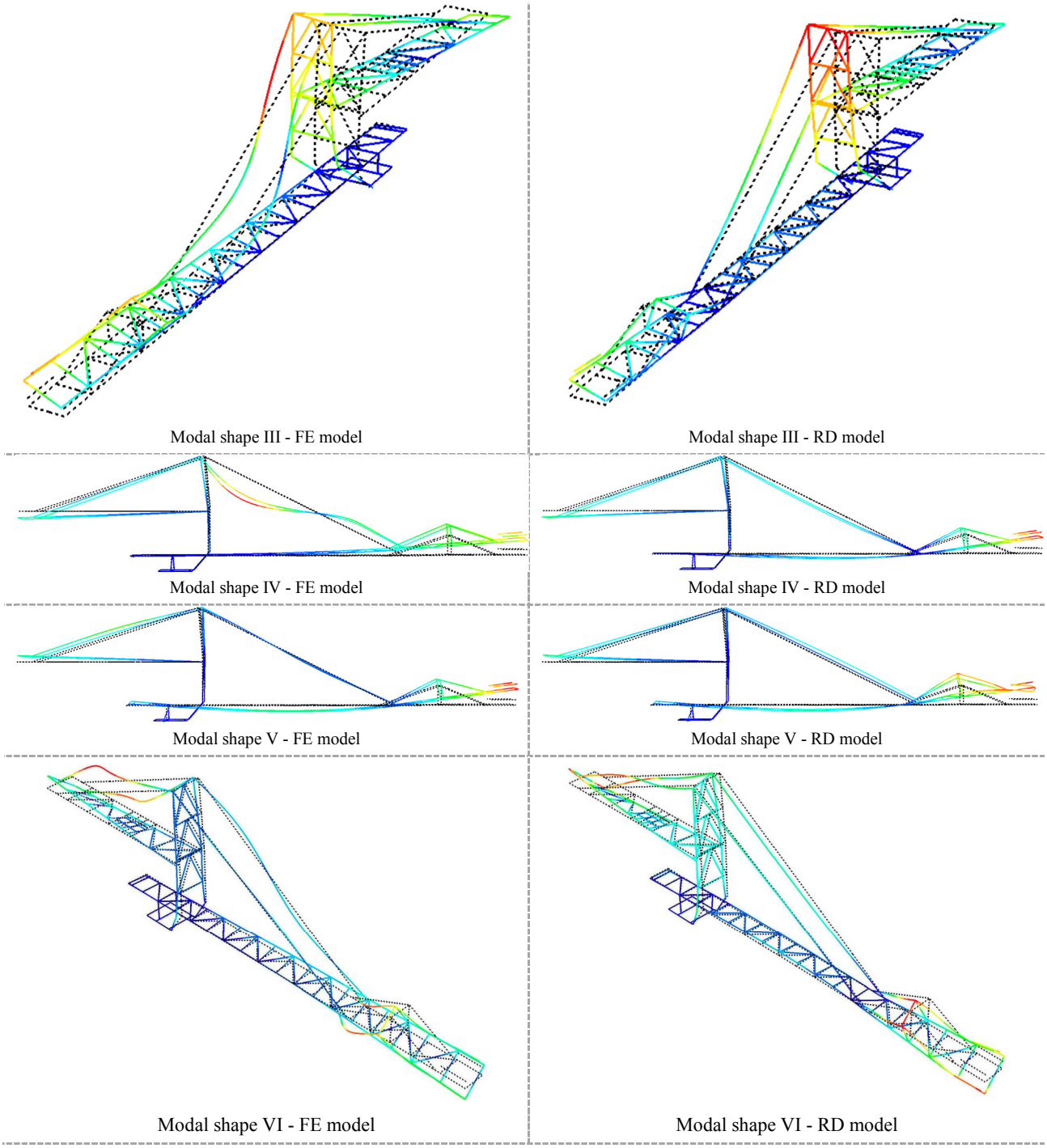

Figure 5. Comparison of FE and RD model modal shapes (part 2)

As can be seen in Table 3, the deviations of the natural frequencies of the RD model in relation to the FE model are less than 5% for the first, second, third, fifth, and sixth natural frequencies. A somewhat larger deviation of 7.42% occurs in the fourth natural frequency, the consequence of this deviation is the impossibility of following the bending of the discharge boom in the vertical plane due to the lack of generalized coordinates in the span part of the boom.

Given such low deviations and the matching of all six modal forms, it can be concluded that the RD model describes the behavior of the system with sufficient accuracy.

As the results of the analysis of the dynamic response of the stacker due to the eccentricity of the tension pulley, the displacements (Figure 6) and accelerations (Figure 7) of the referent points RP1 and RP2 (points of the discharge boom tip), RP7 and RP8 (points of the ballast boom tip), RP11 and RP12 (points of the mast tip), respectively. Due to the extensiveness of the results, displacements and accelerations are shown only in the directions of the generalized coordinates in which they have the highest values. Table 4 shows the corresponding generalized displacements and accelerations of the mentioned RPs, as well as their directions.

Table 4. Maximum generalized displacements and accelerations of the corresponding RPs and their directions

Referent point (RP)	General direction of displacement and acceleration	Generalized displacement	Generalized acceleration	Axis of general coordinate system
RP1	vertical	$u_{\text{ver\_RP1}} = q_2$	$a_{\text{ver\_RP1}} = \ddot{q}_2$	y axis
RP2	vertical	$u_{\text{ver\_RP2}} = q_5$	$a_{\text{ver\_RP2}} = \ddot{q}_5$	y axis
RP7	vertical	$u_{\text{ver\_RP7}} = q_{20}$	$a_{\text{ver\_RP7}} = \ddot{q}_{20}$	y axis
RP8	vertical	$u_{\text{ver\_RP8}} = q_{23}$	$a_{\text{ver\_RP8}} = \ddot{q}_{23}$	y axis
RP11	lateral	$u_{\text{lat\_RP11}} = q_{33}$	$a_{\text{lat\_RP11}} = \ddot{q}_{33}$	z axis
RP12	lateral	$u_{\text{lat\_RP12}} = q_{36}$	$a_{\text{lat\_RP12}} = \ddot{q}_{36}$	z axis

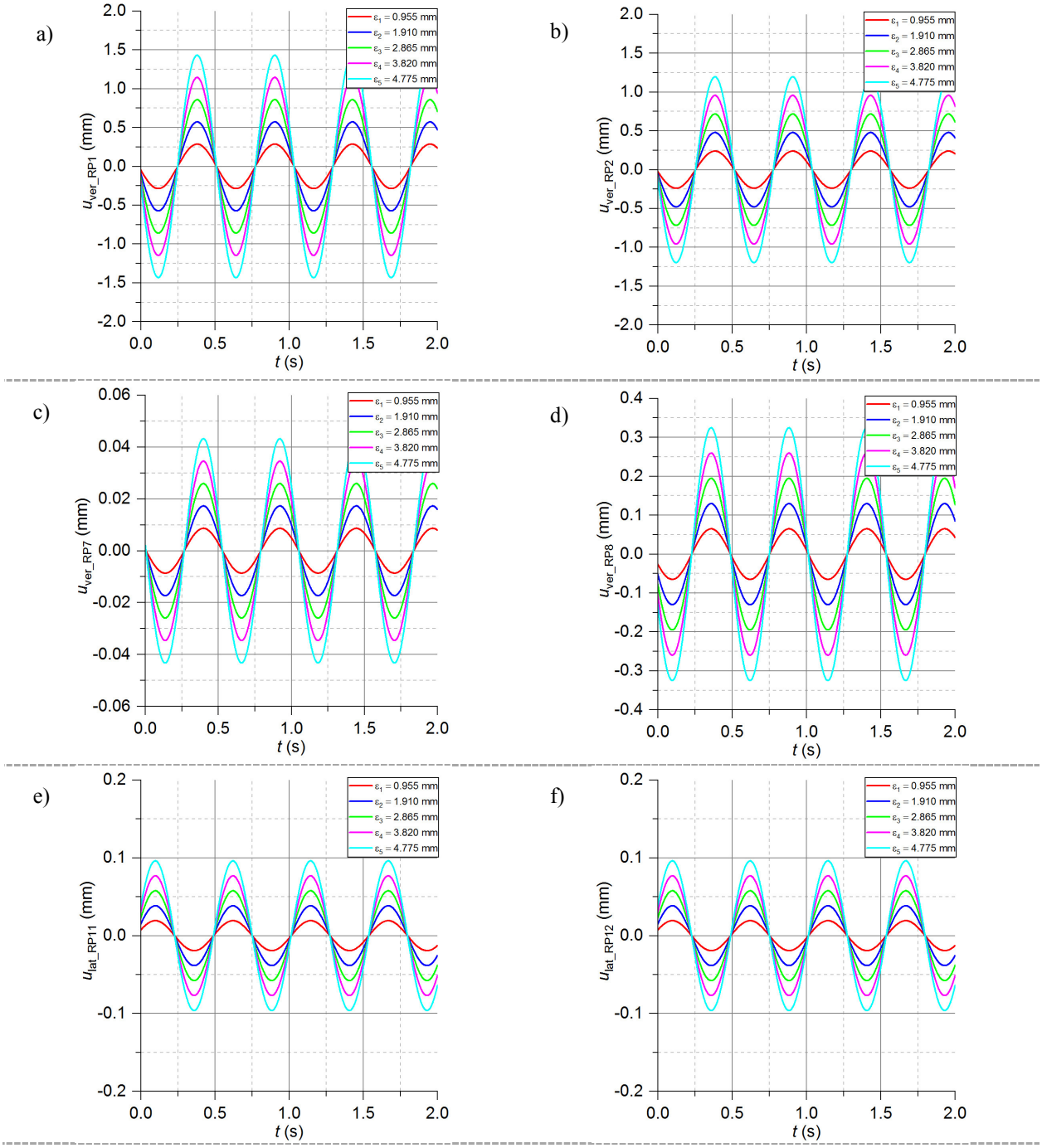

Figure 6. Maximum generalized displacements of the RD model in the corresponding RPs

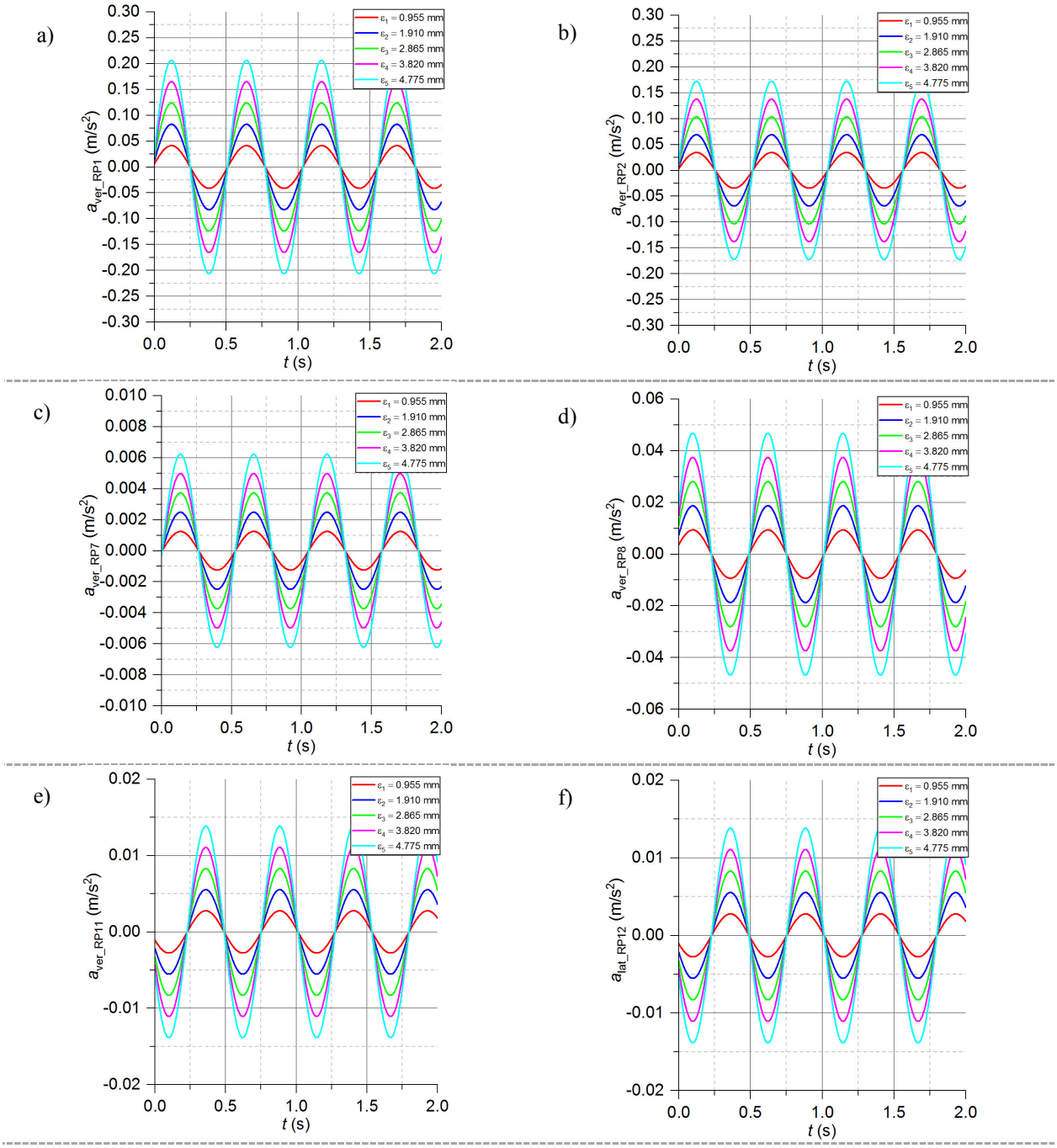

Figure 7. Maximum generalized accelerations of the RD model in the corresponding RPs

4. DISCUSSION

According to the technical regulation [21], the maximum permissible accelerations of the considered RPs are:

- vertical acceleration of the discharge boom tip $a_{\text{v,perm.}}^{\text{disc.boom}} = 1\ \frac{\text{m}}{\text{s}^2}$,
- vertical acceleration of the ballast boom tip $a_{\text{v,perm.}}^{\text{bal. boom}} = 0.5\ \frac{\text{m}}{\text{s}^2}$,
- the lateral acceleration of the mast tip is not defined by the standard,

also, this standard does not prescribe the maximum permissible displacements (deformations) of the bearnig structures of this class of machines.

The values of maximum displacements and accelerations, in all observed RP, were obtained for $\varepsilon_5 = \varepsilon_{\max} = 4.775$ mm, these values are shown in Table 5 and Table 6.

Table 5. The values of the maximum considered displacements of the RPs

RP	$v_{\max}$ (mm)
RP1	$v_{\text{ver\_RP1\_max}} = 1.433$
RP2	$v_{\text{ver\_RP2\_max}} = 1.196$
RP7	$v_{\text{ver\_RP7\_max}} = 0.043$
RP8	$v_{\text{ver\_RP8\_max}} = 0.325$
RP11	$v_{\text{lat\_RP11\_max}} = 0.096$
RP12	$v_{\text{lat\_RP12\_max}} = 0.096$

Table 6. The values of the maximum considered accelerations of the RPs and their comparison with the permissible accelerations

$a_{\max}\ (\mathrm{m/s^2})$	$a_{\text{perm.}}\ (\mathrm{m/s^2})$	$\lambda_a = \frac{a_{\text{perm.}}}{a_{\max}}$
$a_{\text{ver\_RP1\_max}} = 0.206$	$a_{\text{v,perm.}}^{\text{disc.boom}} = 1$	4.85
$a_{\text{ver\_RP2\_max}} = 0.172$	$a_{\text{v,perm.}}^{\text{disc. boom}} = 1$	5.81
$a_{\text{ver\_RP7\_max}} = 0.006$	$a_{\text{v,perm.}}^{\text{bal. boom}} = 0.5$	83.33
$a_{\text{ver\_RP8\_max}} = 0.047$	$a_{\text{v,perm.}}^{\text{bal. boom}} = 0.5$	10.64
$a_{\text{lat\_RP11\_max}} = 0.014$	/	/
$a_{\text{lat\_RP12\_max}} = 0.014$	/	/

The coefficient λ_a shows the ratio of the prescribed permitted accelerations and the values of the maximum accelerations obtained by the dynamic analysis of the system. A low value of this coefficient indicates a greater closeness of the maximum accelerations to the permitted ones, on the basis of which the condition $\lambda_a \geq 1$ must apply.

The vertical acceleration of point RP1 has the lowest value of coefficient λ_a and it is 4.85, which means that acceleration $a_{\text{ver\_RP1\_max}}$ has a value of $\approx 20\%$ of the allowed acceleration, while for point RP2 this coefficient is slightly higher. As the tension pulley is located at the top of the boom, it was expected that the dynamic effects would be most pronounced precisely at these points. The values of the coefficient λ_a for RP7 and RP8 indicate a low value of the vertical acceleration of the ballast boom tip, however, this fact cannot be said to have been expected without a dynamic analysis of the system because the ballast of the stacker, which represents one of the dominant masses, is located exactly in the zone of these points.

Quantification of the influence of the eccentricity value was carried out through the coefficient λ_ε, which represents the ratio of the maximum and minimum acceleration values in a certain RP, that is, the increase in acceleration depending on the eccentricity. Diagrams of acceleration changes at the considered points, depending on the eccentricity, are shown in Figure 8, while the values of the coefficient λ_ε are shown in Table 7.

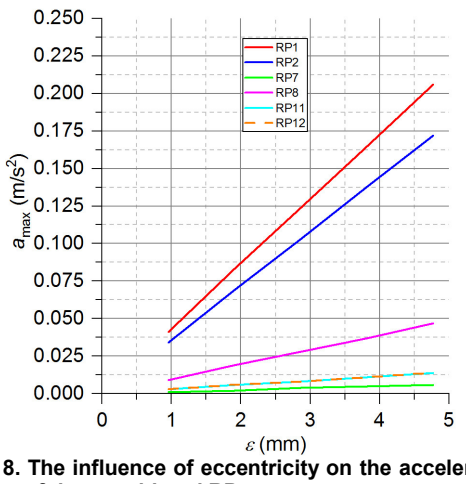

Figure 8. The influence of eccentricity on the accelerations of the considered RPs

Table 7. Values of coefficient λ_ε

RP	$a_{\min}^{\text{RP}}\left(\frac{\text{m}}{\text{s}^2}\right)$	$a_{\max}^{\text{RP}}\left(\frac{\text{m}}{\text{s}^2}\right)$	$\lambda_\varepsilon = \frac{a_{\max}^{\text{RP}}}{a_{\min}^{\text{RP}}}$
RP1	0.041	0.206	5.02
RP2	0.034	0.172	5.06
RP7	0.001	0.006	6
RP8	0.009	0.047	5.22
RP11	0.003	0.014	4.66
RP12	0.003	0.014	4.67

According to Figure 8, it can be observed that the acceleration change trend is linear, also, according to Table 7, it can be observed that the values of the acceleration growth coefficient, in almost all RPs, are around $\lambda_\varepsilon \approx 5$, which also corresponds to the ratio $\varepsilon_{\max}/\varepsilon_{\min} = 5$. Even despite the fact that $\frac{f_{\text{exc}}}{f_6} = 1.04$, the linear trend of acceleration change indicates that the system works out of the resonance region.

5. CONCLUSION

Based on the above, the following conclusions were formed:

- Spatial FE and RD model indicated that the construction in modes I and II oscillates in the horizontal plane, while in mode III torsional oscillation of the outgoing boom occurs (Figure 5). These facts would be oversighted if the system were considered only in the vertical plane. In view of the above, this approach to the formation of the RD model of the stacker superstructure would enable the analysis of the longitudinal eccentricity along the tension drum rotation axis, which would lead to the appearance of additional force couples that would be unevenly distributed on the grooves of the tension pulley and thereby caused additional bending and torsion of the structure;
- Dynamic effects that occur as a consequence of the existence of centrifugal force due to the eccentricity of the tension pulley inevitably exist and cannot be ignored. Considering that in this case only the impact of the eccentricity of the drum that occurs in its production process was analyzed, the acceleration values are not high compared to the permitted values, however, even then, in the area of the discharge boom tip, they can reach 20% of the permitted vertical accelerations for the adopted parameters;
- The technical regulation [23] states that the dynamic loads that occur due to the eccentricity of the rotating masses can be considered as local, as it is confirmed on the basis by the values of the coefficient λ_a shown in Table 6 confirm.

The eccentricities of the pulleys that occurred during the multi-decade exploitation of the machine would inevitably have higher values compared to the eccentricity that occurred during the production of the pulleys, which is within the prescribed tolerances. With that in mind, the coupling of other external dynamic influences with the mentioned eccentricity could potentially lead to the emergence of a more significant response of the structure, as well as to negative dynamic effects that can be reflected on the structure in a global and not only local sense.

ACKNOWLEDGMENT

This work is a result of research supported by the Ministry of Education, Science and Technological Development of the Republic of Serbia by Contract 451-03-68/2022-14/200105.

REFERENCES

[1] Bleck-Neuhaus, J.: Mechanical resonance: *300 years from discovery to the full understanding of its importance*, arXiv:1811.08353v1 [physics.hist-ph], 2018.

[2] Zrnić, N., Bošnjak, S. and Hoffmann, K.: Parameter sensitivity analysis of non-dimensional models of quayside container cranes, Mathematical and Computer Modelling of Dynamical Systems, Vol. 16, No. 2, pp. 145–160, 2010.

[3] Pankratov, S.A.: *Dynamics of the surface mining and earthmoving machines,* Mašinostroenie, Moscow,1967.

[4] Giulia, M., Banisoleiman, K. and Gonzalez, A.: An investigation into the moving load problem for the lifting boom of a ship unloader, Eng. Struct., Vol. 234, pp. 1–20, 2021.

[5] Rasper, L.: *The bucket wheel excavator: Development, design, application*, Trans Tech Publications, Clausthal-Zellerfeld, 1975.

[6] Zrnić, N., Hoffmann, K. and Bošnjak, S.: Modelling of dynamic interaction between structure and trolley for mega container cranes, Mathematical and Computer Modelling of Dynamical Systems, Vol 15, No. 3, pp. 295–311, 2009.

[7] Rusiński, E., Czmochowski, J. and Pietrusiak, D.: Problems of steel construction modal models identification, Eksploat. Niezawodn., Vol 14, No. 1, pp. 54–61, 2012.

[8] Zrnić, N., Gašić, V. and Bošnjak, S.: Dynamic responses of a gantry crane system due to a moving body considered as moving oscillator, Archives of Civil and Mechanical Engineering,Vol. 15, No.1, pp. 243–250, 2015.

[9] Zrnić, N., Gašić, V., Urosevic, M. and Arsic, A.: Finite Element and Analytical Modelling of Ship Unloader, X International Conference "Heavy Machinery-HM 2021", Vrnjačka Banja, 23–25 June, pp. A.13-A.18, 2021.

[10] Gašić, V., Zrnić, N. and Rakin, M.:Consideration of a moving mass effect on dynamic behaviour of a JIB crane structure | Analiza utjecaja pokretne mase na dinamičko ponašanje konstrukcije stupne konzolne dizalice, Tehnicki Vjesnik, Vol. 19, No.1, pp. 115–121, 2012.

[11] *Coal industry across Europe*, 7th ed. Brussels: EURACOAL AISBL - European Association for Coal and Lignite, 2020.

[12] Production of electricity. Belgrade: Electric Power Industry of Serbia (EPS), http://www.eps.rs/eng/Poslovanje-EE.

[13] *Energy sector development strategy of the Republic of Serbia for the period by 2025 with projections by 2030*, Belgrade: Ministry of Mining and Energy, 2016.

[14] Rusiński, E., Czmochowski, J., Moczko, P. and Pietrusiak, D.: *Surface Mining Machines - Problems of Maintenance and Modernization*, Springer International Publishing AG, 2017.

[15] Pantelić, M., Bošnjak, S., Misita, M., Gnjatović, N. and Stefanović, A.: Service FMECA of a bucket wheel excavator, Eng. Fail. Anal. Vol. 108, 2020.

[16] Schmidt, M. J.: *Structural failures on mobile materials handling equipment*, Dissertation for the degree of Master of Science, Faculty of Engineering, University of Pretoria, 2014.

[17] Bugarić, U., Tanasijević, M., Polovina, D., Ignjatović, D. and Jovancic, P.: Lost production costs of the overburden excavation system caused by rubber belt failure, Eksploat. Niezawodn.,Vol. 14, No.4, pp. 333–341, 2012.

[18] Volkov, D.P. and Cherkasov, V.A.*: Dynamics and strength of multi-bucket excavators and stackers*, Mašinostroenie, Moscow, 1969.

[19] Smolnicki, T., Kowalczyk, M. and Pietrusiak, D.: Identification of dynamic characteristics of the stacker, 6th International Conference MECHATRONIC SYSTEMS AND MATERIALS, Opole, Poland 5-8 July, 2010.

[20] Pietrusiak, D., Moczko, P., Smolnicki, T. and Rusiński, T.: Identification of low cycle dynamic loads acting on heavy machinery, X International Conference on Structural Dynamics, EURODYN 2017, Vol 199, pp. 254-259, 2017.

[21] DIN 22261-2, *Excavators, spreaders and auxiliary equipment in brown coal opencast lignite mines - Part 2: Calculation Principles*, German Institute for Standardization, Berlin, 2016.

[22] AS4324.1, *Mobile equipment for continuous handling of bulk materials - Part 1: General requirements for the design of steel structures*, Standards Australia, Homebush (NSW), 2017.

[23] FEM 2 131/2 132: *Rules for the design of mobile equipment for continuous handling of bulk materials*, France, 1997.

[24] Jiang, Y. Z., Liu, C. J., Li, X. J., He, K. F., Xiao and D. M.: Low-Frequency Vibration Testing of Huge Bucket Wheel Excavator Based on Step-Decay Signals, Shock and Vibration, Vol. 2018, pp. 1-7, 2018.

[25] Bošnjak S., Oguamanam D. and Zrnić N.: On the dynamic modeling of machines: Part I - Bucket wheel excavators, Proceedings of the 18th International Conference on Material Handling Constructions and Logistics MHCL 2006, pp. 13-28, Belgrade, 2006.

[26] Bošnjak, S., Oguamanam, D. and Zrnić, N.: The influence of constructive parameters on response of bucket wheel excavator superstructure in the out-of-resonance region, Arch. Civ. Mech. Eng., Vol 15, No. 4, pp. 977–985, 2015.

[27] Gnjatović, N., Bošnjak, S. and Zrnić, N.: Spatial reduced dynamic model of a bucket wheel excavator with two masts, Proceedings of the 14th International Scientific Conference: Computer Aided Engineering (CAE 2018), Wroclaw (Poland), 2018, Lecture Notes in Mechanical Engineering, Springer, Cham, pp. 215–235, 2019.

[28] *Belt conveyors for bulk materials*, Chapter 14, Conveyor Equipement Manufacturers Association (CEMA), Naples, Florida, USA, 2005.